Experiments on Magnetically Driven Superflow in ^{3}He-A_1

R. Ruel and H. Kojima
Serir Physics Laboratory, Rutgers University, Piscataway, New Jersey 08854
(Received 7 March 1985)

Magnetically generated superflows were observed in the ^{3}He-A_1 phase at pressures of 22.3 to 25.9 bars in magnetic fields of 3.7 to 5.5 kG. A two-fluid model is used to calculate the magnitude of the magnetic fountain effect. Critical-velocity effects were observed for sufficiently high flow rates. The critical velocity in the ^{3}He-A_1 phase was found to be 0.21 mm/sec in the reduced temperature range 0.0004 to 0.008. A threshold field gradient for the magnetic fountain effect was observed in part of the A_1 phase and may be evidence of fluctuations above T_{c2}.

PACS numbers: 67.50.Fi

When liquid ^{3}He is cooled in a strong magnetic field, it first undergoes a second-order transition into the superfluid A_1 phase.[1] The phase diagram of the A_1 phase was recently studied by Israelsson *et al.*[2] and by Sagan *et al.*[3] A unique hydrodynamic mode exists in the A_1 phase as a consequence of its broken relative-spin–gauge symmetry. Liu[4] derived the equation of motion of the superfluid component of the A_1 phase given in linearized form by

$$\partial \mathbf{v}_s/\partial t = -[\nabla\mu + M_s(\hbar/2m)\nabla\omega], \quad (1)$$

where v_s is the velocity of the superfluid component, μ is the chemical potential, $\hbar$ is Planck's constant divided by 2π, m is the mass of the ^{3}He atom, and M_s $(=-1)$ is the magnetic quantum number[4,5]; $\omega=\gamma(\gamma S/\chi - H)$, where γ is the gyromagnetic ratio, χ is the magnetic susceptibility, S is the spin angular momentum per unit volume, and H is the externally applied magnetic field. The chemical-potential term allows the possibility of thermally driven superflow (as in the fountain effect in ^{4}He); the $\nabla\omega$ term makes it possible to generate a superflow by applying a magnetic field gradient. This hydrodynamic mode was first observed as a spin-temperature wave in ^{3}He-A_1 by Corruccina and Osheroff[6] in 1980. We previously reported on the determination of the direction of the magnetization of the superfluid component of the A_1 phase by observation of the pressure gradients produced by applying static magnetic field gradients across a superleak.[5]

In this paper we present the results of a systematic study of the magnetically driven superflows in the A_1 phase generated by transiently or sinusoidally (frequency 0.5 to 3.0 Hz) applying a magnetic field gradient across a superleak. The observed magnitude of the superflow is in good agreement with the magnetic fountain effect predicted by Liu.[4] When a sufficiently large magnetic field gradient is applied, critical velocity effects are observed. An unusual nonlinear behavior in the oscillatory response is observed in the low-temperature region of the A_1 phase: A threshold magnetic field gradient exists below which apparently no superflow is generated.

The heart of our experiment is a differential pressure sensor which detects the difference in liquid-^{3}He pressure between a small chamber and a liquid reservoir connected by a superleak. A schematic of the sensor is shown in Fig. 1. A stack of ten rectangular channels, each having the dimensions $6.5\times0.025\times3.3$ mm^3 ($\hat{\mathbf{x}},\hat{\mathbf{y}},\hat{\mathbf{z}}$ axes), acts as a superleak which connects the liquid reservoir above the sensor and a small closed chamber (volume of 4.0×10^{-3} cm^3) just below it. The lower wall of the chamber is a flexible, silver-coated, 5-μm-thick polycarbonate diaphragm. The movable diaphragm, together with the silver coating on the lower face of the wall containing the superleak channels, constitute two plates of a capacitively detected differential pressure sensor (plate separation of 70 μm, ambient capacitance of 7.6 pF). The region below the diaphragm is connected to the liquid reservoir via four relatively large channels surrounding the sensor. The effective tension of the diaphragm was measured electrostatically at 25 mK with the sensor immersed in liquid ^{3}He and was found to be 2.6×10^5 dyn/cm. A static magnetic field up to 5.8 kG $\hat{\mathbf{z}}$ could be applied in the sensor region using a superconducting magnet. The magnetic field was homogeneous within 0.1%

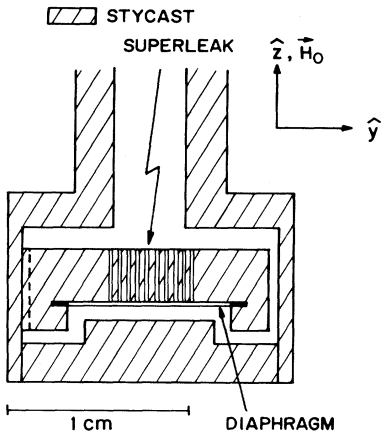

FIG. 1. The superleak differential-pressure-sensor assembly.

along the superleak and 2% radially inside the volume of the differential pressure sensor. The magnetic field gradient to drive the superfluid was provided by a pair of oppositely wound coils. The magnetic field gradient per unit current was measured to be 33 G/cm · A.

The method of cooling the liquid ^{3}He is the same as reported in our previous paper.[5] However, a significant improvement was made to the thermometry by placing the thermometer much closer to the sensor than previously. The magnetic susceptibility of La-diluted cerium magnesium nitrate powder measured by a SQUID-based mutual-inductance bridge was calibrated against an independently calibrated germanium-resistance thermometer in the range between 0.3 and 1.0 K. The La–cerium-magnesium-nitrate pill was thermally linked to the differential pressure sensor region by a 6-cm liquid-^{3}He column of diameter 4.0 mm. The transition temperature, T_c^*, measured by our thermometer at $P=22.3$ bars, is 2.361 mK. This value may be compared with $T_c^*=2.433$ mK determined by zero sound attenuation by Paulson *et al.*[7] Our magnetic temperatures were converted to the La Jolla temperature scale by comparing measurements of T_c^* at different pressures in the range 22.3 to 25.9 bars.

A simple two-fluid model is used to describe the sensor response. Consider the differential pressure sensor shown in Fig. 1. In the very low-frequency range of our measurements, all inertial terms may be neglected. The average displacement z of the diaphragm (area B) is related to its tension σ and the differential pressure δP across the superleak by

$$8\pi\sigma z - B\delta P = 0. \tag{2}$$

Equation (1) yields

$$\frac{\delta P}{\rho L} + M_s \frac{\hbar\gamma}{2mL}\left(\frac{\gamma\delta S}{\chi} - \delta H\right) = 0, \tag{3}$$

where δ(quantity) is the difference in the quantity across the superleak of length L and ρ is the mass density. The equation of motion for the normal fluid (velocity v_n and density ρ_n) in the superleak channel is

$$\delta P/\rho L + R v_n = 0, \tag{4}$$

where R, the flow resistance, is $12\eta/\rho h^2$ (h is the height of the superleak channels and η the shear viscosity). The fluid motion in the low-frequency range of our experiment may be considered incompressible and we can write a continuity equation

$$\rho B\dot{z} = (\rho_s v_s + \rho_n v_n) A, \tag{5}$$

where A is the total cross-sectional area of the superleak, ρ_s the superfluid density, and v_s the superfluid velocity. The time rate of change of spin density in the chamber between the capacitor plates is

$$\delta\dot{S} = M_s(\hbar/2m)\rho_s v_s (A/V), \tag{6}$$

where V is the volume of the chamber. The longitudinal relaxation time T_1 is long compared to the time scale of the measurements[8] and therefore the changes in the spin density are governed by the mass flow. Equations (2) to (6) will be used to model the experimental results. The effects of the finite longitudinal relaxation time, the connecting channels in parallel with the superleak, and spin diffusion do not significantly change the prediction of this model.

In the inset to Fig. 2 we show an example of the response of the differential pressure sensor in the A_1 phase at a pressure of 22.3 bars and in a static magnetic field of 5.52 kG when the magnetic field gradient is increased linearly from −33 to +33 g/cm (along $\hat{\mathbf{z}}$) in a ramp time of 100 msec. The field gradient is left constant for 10 sec, which is sufficiently long for observing the transient response. The capacitance of the differential pressure sensor is recorded and averaged. The response is plotted as the displacement of the diaphragm as a function of time. The observed direction of displacement agrees with our previous identification that the magnetic moment of the paired spins of superfluid-A_1 phase is aligned in the same direction as the applied static field. The relaxation of this pulse is an exponential with a decay-time constant of 440 msec.

A series of these measurements was taken as the temperature drifted through the A_1 phase at a rate of about 30 μK/h. The measured temperature depen-

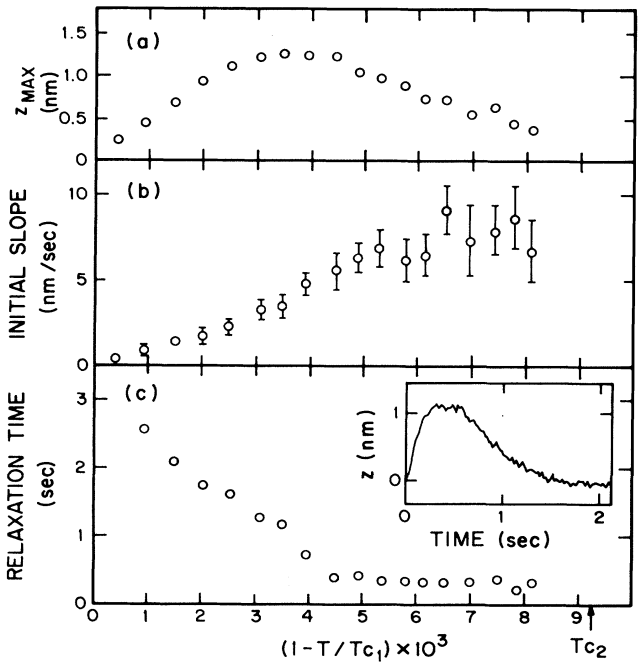

FIG. 2. Characteristics of the pressure-sensor response as a function of reduced temperature. Inset: a typical response. This plot is an average of 32 pulses; the decay time constant is 440 msec.

dence of the peak displacement (z_{max}), initial slope, and the decay-time constant are shown in Figs. (2a), (2b), and 2(c), respectively, as a function of reduced temperature $t=1-T/T_{c1}$. The liquid pressure was 22.3 bars, the static magnetic field was 5.52 kG, and the ramp time was 40 msec for the data shown in Fig. 2. The temperature shown as T_{c2} in the graph is the transition temperature we observed in the ac experiments discussed below. The observed temperature dependence of the initial slope in Fig. 2(b) may be understood in terms of a critical velocity effect. The slope of a pulse is related to the volume flow rate of fluid through the superleak. The 40-msec ramp time for the data in Fig. 2(b) is short enough that the critical velocity is reached in the superleak channels during the ramp up. If the critical velocity is independent of temperature, the critical flow rate is proportional to the superfluid fraction, which in turn is proportional to the reduced temperature $[\rho_{s\perp}/\rho=0.2(1-T/T_{c1})]$ (Ref. 6). A straight-line fit to the data of Fig. 2(b) gives a critical velocity of 0.21 ± 0.04 mm/sec.

When we solve Eqs. (2)–(6) for the diaphragm displacement $z(t)$ for our transient experiment, we find that after the magnetic field gradient becomes constant, the diaphragm displacement should decay exponentially. The calculated value of the pressure relaxation-time constant is about 325 msec at T_{c1} and decreases about 25% through the A_1 phase because of decreasing normal-fluid shear viscosity.[9] The origin of the long decay time just below T_{c1} seen in Fig. 2(c) is not understood. We do not believe that the increased relaxation time is a second viscosity effect.[10] An additional dissipation due to second viscosity would result in a marked temperature dependence near T_{c1} of the magnitude of the magnetic-fountain-effect signal in our ac experiments. In these experiments described below, we observe a temperature-independent amplitude in the region near T_{c1}.

The measured temperature dependence of the diaphragm response to sinusoidally applied magnetic field gradients at a ^{3}He pressure of 22.3 bars and static field of 4.66 kG is shown in Fig. 3. For all the data shown in Fig. 3, the frequency of oscillation was 0.75 Hz. The results in Fig. 3 were read from a chart recording of the amplitude of the capacitance oscillations taken while drifting through the A_1 phase with the amplitude of the sinusoidal magnetic field gradient kept constant. For sufficiently small warm-up rates, the measured temperature dependence of the response did not significantly depend on the warm-up rate. The maximum temperature interval, $T_{c1}-T_{c2}$, does not depend either on the frequency of oscillation or peak-to-peak gradient coil current (i) for $i\geq 2.0$ A. We identify the temperature at which the response for $i\geq 2.0$ A vanishes as T_{c2}. The width of the A_1 phase measured in this manner is 4.3 μK/kG. This width is somewhat smaller than the width of 4.95 μK/kG reported in Ref. 2 at this pressure.

As is clear from Fig. 3, the oscillatory response may be divided into two distinct regions of temperatures: above and below $t=3\times10^{-3}$. In Fig. 4 the displacement amplitudes at given values of reduced temperature below $t=3\times10^{-3}$ are taken from Fig. 3 and shown as a function of the current in the field gradient coil. It can be seen from Fig. 4 that in this temperature range the displacement amplitude at a given temperature increases linearly with the applied field gradient amplitude until a critical value is exceeded. Then the response deviates from the linear behavior. The slope of the linear region in Fig. 4 is independent

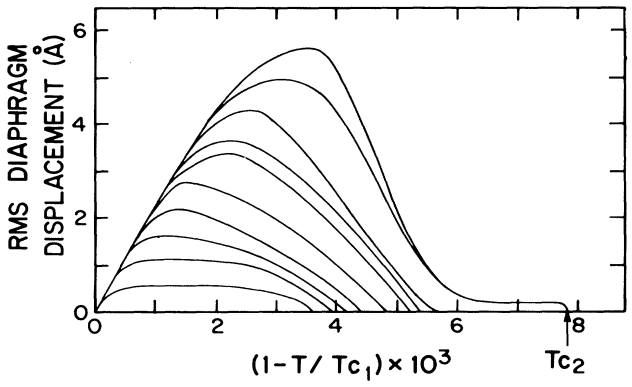

FIG. 3. Pressure sensor response at several different amplitudes of sinusoidal applied field gradient. The peak-to-peak gradient coil currents are 0.2, 0.4, 0.6, 0.8, 1.0, 1.2, 1.4, 1.8, 2.0, and 2.4 A for the smallest to the largest response, respectively. The noise of these signals is not shown; the superimposed noise is about 0.1 Å.

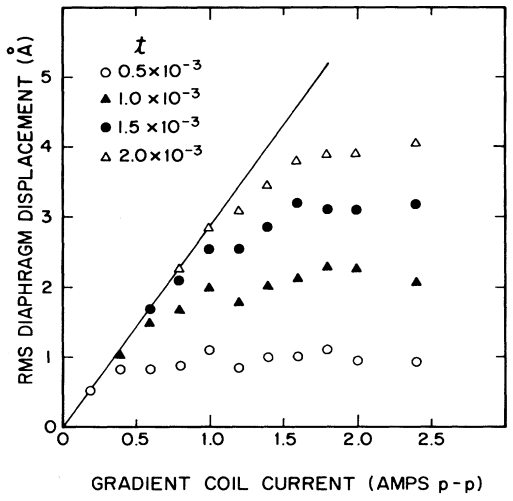

FIG. 4. Pressure-sensor response at several values of reduced temperature.

of temperature as well as the static field and its value is 2.9 Å/A. This slope is essentially the magnitude of the magnetic fountain effect. Solving Eqs. (2)–(6) by assuming a sinusoidal solution $\delta H = H_0 e^{i\omega t}$ and $\delta z = z_0 e^{i\omega t}$ we obtain

$$|z_0| = \frac{(V\chi m/B\rho\mu)\omega\delta H_0}{[(1+X)^2\omega^2 + Y^2]^{1/2}}, \tag{7}$$

where

$$\mu = \frac{\hbar\gamma}{2}, \quad X = \frac{8\pi\sigma\chi m^2 V}{\rho^2\mu^2 B^2}, \quad Y = \frac{\rho_n A 8\pi\sigma}{\rho^2 B^2 LR}.$$

Evaluation of Eq. (7) at 22.3 bars gives a slope of 1.60 Å/A, which is a factor of 0.56 times the measured slope. We regard the difference to be within the uncertainties of the volume, flow resistance, and the diaphragm tension and that our results confirm the magnitude of the magnetic fountain effect predicted by Liu.[4]

We interpret the response in Fig. 4 where the displacement deviates from linear behavior as a critical-velocity effect. Assuming the critical velocity is reached in the superleak channels, we calculate a critical velocity of 0.22 ± 0.02 mm/sec at the reduced temperatures in Fig. 4. The magnitude of the critical velocity did not depend on the applied static field between 3.7 and 5.5 kG.

In the temperature range $t > 3\times10^{-3}$, an unusual nonlinear behavior is seen in Fig. 3. The displacement amplitude is very small or zero within the noise up to a temperature-dependent threshold value of the magnetic field gradient. Once the threshold field gradient is exceeded, the displacement amplitude increases as the field gradient is increased with a temperature-dependent slope. To check if these effects might be caused by a changing temperature gradient between the sensor and the thermometer, we measured the response as a function of applied field gradient as t was held constant at several different values. These measurements with stabilized temperature reproduced the behavior shown in Fig. 3.

A possible explanation for the threshold effect is that of fluctuations above T_{c2} (see, for example, Patton[11]). As pointed out by Liu[12] a small amount of up-spin superfluid would be very effective in reducing the magnetic fountain effect in the down-spin superfluid-A_1 phase. Similar small fluctuations around T_{c1} would not be seen in our capacitance signal. These values are taken from data in Fig. 3. A comparison of ac experiments performed in different magnetic fields shows that the threshold effect begins at about 10 μK above T_{c2} regardless of the width of the A_1 phase. This is further evidence that the threshold effect is a precursor of T_{c2}.

We thank Anthony Leggett and Mario Liu for several helpful discussions and Chris Gould for a very useful preprint. One of us (R.R.) received partial financial support from RCA during the course of this work. This research was supported in part by a Research Council Grant from Rutgers University.

[1]W. J. Gully, D. D. Osheroff, D. T. Lawson, R. C. Richardson, and D. M. Lee, Phys. Rev. A **8**, 1633 (1973).
[2]U. E. Israelsson, B. C. Crooker, H. M. Bozler, and C. M. Gould, Phys. Rev. Lett. **53**, 1943 (1984).
[3]D. C. Sagan *et al.*, Phys. Rev. Lett. **53**, 1939 (1984).
[4]M. Liu, Phys. Rev. Lett. **43**, 1740 (1979).
[5]R. Ruel and H. Kojima, Phys. Rev. B **28**, 6582 (1983).
[6]L. R. Corruccini and D. D. Osheroff, Phys. Rev. Lett. **45**, 2029 (1980).
[7]D. N. Paulson *et al.*, J. Low Temp. Phys. **34**, 63 (1979).
[8]L. R. Corruccini and D. D. Osheroff, Phys. Rev. Lett. **34**, 564 (1975).
[9]T. A. Alvesalo *et al.*, J. Low Temp. Phys. **19**, 1 (1974).
[10]H. Brand and M. C. Cross, Phys. Rev. Lett. **49**, 1959 (1982).
[11]B. R. Patton, Phys. Lett. **47A**, 459 (1974).
[12]M. Liu, Physica (Utrecht) **109&110B**, 1615 (1982).